ELSEVIER

Journal of Nuclear Materials 313–316 (2003) 469–477

journal of nuclear materials

www.elsevier.com/locate/jnucmat

Section 5. Plasma fueling, hydrogen isotope behavior, recycling and tritium

Deuterium retention in tungsten in dependence of the surface conditions

O.V. Ogorodnikova *, J. Roth, M. Mayer

Max-Planck-Institut für Plasmaphysik, EURATOM Association, Boltzmannstraße 2, D-85748 Garching, Germany

Abstract

The paper reviews hydrogen isotope retention and migration in tungsten (W). Due to a large scatter of the deuterium (D) retention database, new measurements of ion-driven D retention in polycrystalline W foil have been performed to clarify the mechanism of hydrogen isotope inventory in W. Deuterium retention has been investigated as a function of ion fluence, implantation temperature, incident energy and surface conditions. Special attention has been given on the investigation of D retention in thin films of tungsten carbide and tungsten oxide which can be formed on W surface in a fusion device. Such kinds of films increase the D retention in W. Several points are reviewed: (i) inventory in pure W, (ii) inventory in W pre-implanted by carbon ions and (iii) inventory in tungsten oxide.

PACS: 52.40.Hf
Keywords: Deuterium; Tungsten; Retention; Implantation

1. Introduction

Plasma-facing materials for in-vessel components of fusion reactors should satisfy the following criteria: good thermal properties (high melting point and high thermal conductivity), good mechanical properties (low crack growth rate under cyclic stresses), low erosion, low hydrogen isotope permeation and inventory and low activation by neutrons. Tungsten (W) has a high melting temperature and a high threshold energy for physical sputtering and is considered as one of the plasma-facing materials for fusion devices.

For the safety reason, it is important to understand the behaviour of hydrogen isotopes in W. However, instead of the increase of publications about hydrogen isotope transport in W, the physical mechanism of hydrogen trapping and migration in W is not completely understood yet. The experimental data of hydrogen retention and release for W are rather limited and partly contradictory [1–14]. Although most of the variation in the experimental data can be traced back to various methods of measurements, experimental conditions and differences in the specimen preparation, it is still not clear which data are more reliable for the prediction of the tritium inventory in pure W for fusion applications.

In the present ITER design, carbon fiber composites, beryllium and W are proposed to be used as plasma-facing materials. Physical and chemical sputtering by fast deuterium and tritium ions and charge-exchange neutral atoms causes erosion of plasma-facing materials, deposition of one construction material on another and creation of mixed layers. Additionally, the presence of impurities, for example oxygen, in the plasma may modify the material surface and induce a higher inventory of hydrogen isotopes. The database for deuterium (D) retention in mixed materials is still scarce. Only a few data have been reported on D retention in W pre-implanted by carbon ions [15,16] and tungsten oxide [17]. Whereas reliable data on the hydrogen isotope behaviour in mixed materials like carbides, carbon-containing tungsten and tungsten oxide are of great importance for the prediction of tritium inventory in the components of fusion reactors.

* Corresponding author. Tel.: +49-89 3299 1606; fax: +49-89 3299 2279.
E-mail address: olga.ogorodnikova@ipp.mpg.de (O.V. Ogorodnikova).

0022-3115/03/$ - see front matter
PII: S0022-3115(02)01375-2

Consequently, there is a need for a systematic study of the D retention in both pure polycrystalline W (PCW) and complex W materials. For this reason, in addition to previous experiments, thermal desorption spectroscopy (TDS) measurements for implanted PCW foils to quantify the D retention as a function of ion fluence, implantation temperature, and the presence of carbon and oxide impurities or thin layers on the surface have been done. General results of previous studies for pure and complex W materials indicate the following:

- Implanted D is trapped with trapping energies of 0.5–0.9 and 1.2–1.5 eV [4,5,11,12]. The origin of these traps is not clearly understood. There are also traps with energies of 2–4 eV which are associated with chemical bonding to carbon [6].
- Pre-implantation by He^+ ions results in the production of voids where D can be trapped with the trapping energy about 1.4 eV and chemisorbed on bubble walls with 1.8–2.1 eV [18,19].
- Deep transport and trapping of hydrogen by intrinsic defects far beyond the implantation zone even at room temperature have been observed in [2,3].
- Hydrogen inventory in PCW strongly depends on material structure and the presence of impurities [1,6,10].
- For W pre-implanted with low fluence carbon ions and then implanted with D ions with the range confined within the carbon modified layer, it has been found that D retention in carbon-implanted W can be smaller than that in pure W [15,16].
- Blisters can be formed in W, even if the ion energy is too low to create displacement damage such as vacancies. The studies by Sze and co-workers [22–24], Haasz et al. [9], Venhaus et al. [21] and Wang et al. [20] have demonstrated that hydrogen isotope implantation in W can definitely produce blistering. The nature of blistering is not well understood yet and requires future investigations.

2. Experiments

2.1. Specimens

PCW samples produced for ITER by PLANSEE were cut from relatively high purity foil (99.96% W by weight), a reduced-rolled, power-metallurgy product with principal chemical impurities: O (345), C (460), N (263), H (920), Fe (212), Mo (438), P (613), Si (262), Ca (92), Na (167) on an atomic parts per million (appm) basis. The dimension of the samples was $12 \times 15 \times 0.5$ mm^3. The grain sizes were estimated to be in the range of 1–10 μm. All specimens were mechanically polished and outgased at 1273 K for 10 min in the implantation chamber just before implantation. Some of the specimens were electrochemically polished in 1 wt% NaOH aqueous solution (1 wt% NaOH, 10 V, Pt cathode, 2.5 min at room temperature). Before and after each electropolishing step the samples were weighted on an analytical balance and the etching depth was estimated from the weight loss with an accuracy of about 40%. This indicates the removal of >0.5 μm of the surface layer. The uniformity of the electrochemical etching was controlled by a scanning electron microscopy. With this polishing treatment, the previous implantation zone was removed. Consequently, any memory effect of the previous implantation as was observed in [8] was eliminated.

Various pre-implantation treatments were used:

1. Only heating for 10 min at 1273 K in an implantation chamber with a residual pressure of $p = 10^{-6}$ Pa to remove residual stresses and residual bulk hydrogen (all samples).
2. Bombardment with 600 eV D_3^+ at 1173 K with a residual pressure of $p = 10^{-5}$ Pa for 1 h in order to avoid W oxide layer on the surface.
3. Annealing at 1273 K in an implantation chamber with a residual pressure $p = 10^{-6}$ Pa for 1 h to reduce the intrinsic defect concentration.
4. Annealing at 1573 K for 3 h in a vacuum with a background pressure of $p = 2 \times 10^{-4}$ Pa during annealing. Tungsten tends to re-crystallize under these conditions, i.e. larger grains grow. This temperature is high enough to remove any electro-polish residue from the surface, as well as some impurities, vacancies and dislocations near the surface and to reduce the concentration of dislocations and grain boundaries in the bulk [10].

2.2. Implantation

Deuterium implantation was performed in an ultra-high vacuum accelerator facility using D_3^+ ions at normal incidence to the test specimen. As a source of carbon and oxygen ions, CO_2 with minor additions of H_2 is used.

A pressure of about 10^{-6} Pa is reached. During implantation the pressure increases to $(5–7) \times 10^{-6}$ Pa, mainly due to the partial pressure of the working gas. A liquid N_2 (LN_2) cold finger was installed in the target chamber to reduce the hydrocarbon and water partial pressures, thus minimize the surface contamination during implantation.

2.3. Thermal desorption spectroscopy

The retention of D implanted into pure W and W containing carbon or oxygen in the surface layers was investigated by TDS measurements. The re-emission and TDS experiments were performed at Garching in the high-current ion source for light ions such as H, He, O

and C at energies between 60 eV and 5 keV described in [25]. TDS measurements were done in the same chamber as for implantation just 5 min after the ion beam switch off.

The amount of retained D was measured by TDS with a maximum temperature of 1373 K and a heating rate of 8 K/s. The samples were heated by electron bombardment from outlet side. The target temperature was measured with an error of ±50 K by means of an infrared pyrometer placed outside the chamber. The released particles H_2, HD and D_2 were detected with Balzers 511 quadrupole mass spectrometer (QMS). To reduce the background level (especially, H_2O), the quadrupole ion source is separately pumped and surrounded by a liquid nitrogen cooled copper shield.

The QMS signal was calibrated by implantation of 3 keV D_3^+ in Ti at room temperature with a fluence $F = 10^{22}$ D/m^2. Under these conditions, all non-reflected D is retained in Ti that was detected by TDS.

3. Results and discussion

3.1. D^+ implantation into pure W

3.1.1. Experimental results

Fig. 1 shows the thermodesorption spectra after the implantation of 200 eV D^+ at room temperature in PCW heated at different temperatures before implantation: at 1173 and 1273 K for 1 h in a good vacuum of $p = 10^{-6}$ Pa and at 1573 K for 3 h in a vacuum with a background pressure of $p = 2 \times 10^{-4}$ Pa. TDS clearly demonstrates the decrease of the retention with pre-implantation annealing. TDS for PCW implanted by D at room temperature has two peaks: a low-temperature peak with a maximum about 450 K and a high-temperature peak with a maximum about 600 K. The annealing results in a reduction of the D concentration in the low-temperature peak which can be associated with trapping in 'natural' defects. The annealing at 1173 K for 1 h is not sufficient to significantly change the initial concentration of intrinsic defects like dislocations and grain boundaries. Consequently, the amount of the retained D in such samples is the highest. The increase of the temperature and the time of annealing tends to re-crystallize PCW, i.e. for the temperature of 1573 K and the time of 3 h a growth of grain size was observed by SEM. The grain sizes before and after annealing were approximately 1–5 and 5–15 μm, respectively. This means that the concentration of grain boundaries decreases. The annealing also removes some impurities, vacancies and dislocations in the near the surface. For the samples annealed at 1573 K for 3 h, dislocation and grain boundaries densities near the surface were effectively reduced and the lowest D concentration was observed.

Fig. 2 shows the fluence dependence of the retained D at room temperature in PCW for different pre-implantation treatments. The scatter of the data is likely due to the difference in the initial amount of surface impurities, grain boundaries and dislocations. Because of the low solubility [26] and strong trapping, a small change of the defect concentration can strongly influence the D retention in W. Despite of the scatter of the experimental data, the tendency of the D retention in pure W is clear: the retention increases slightly faster than the square root of the fluence. The same tendency was found by Causey and co-workers [21] (Fig. 3). van Veen et al. [19] reported that the hydrogen retention increases as a square root of the dose. As can be seen in Fig. 4, our data for 500 eV D^+ implantation in PCW are in good agreement with Anderl et al. [6] but in disagreement with Haasz et al. [8] who found a saturation of the D retention at a level of 5×10^{20} D/m^2 already at a fluence $F = 10^{23}$ D/m^2. The purity of the PCW was the same in our experiments and

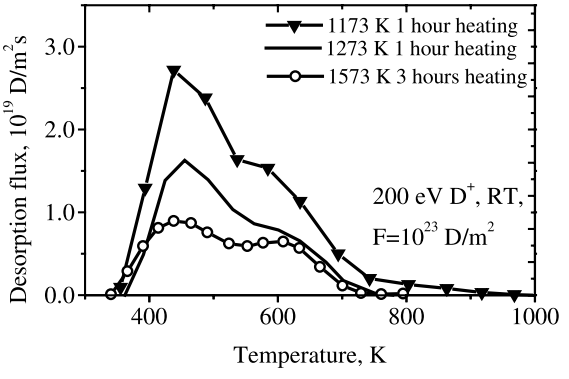

Fig. 1. Thermodesorption spectra for 200 eV D^+ implanted in PCW at room temperature and fluence $F = 10^{23}$ D/m^2 for various pre-implantation annealing.

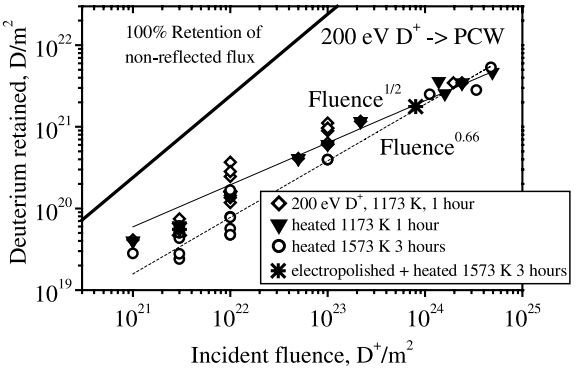

Fig. 2. Fluence dependence of the retained D under the implantation of 200 eV D^+ in PCW at room temperature. Various conditions of pre-implantation treatment are shown. The reflection coefficient of 200 eV D^+ from W is $r = 0.56$ [27].

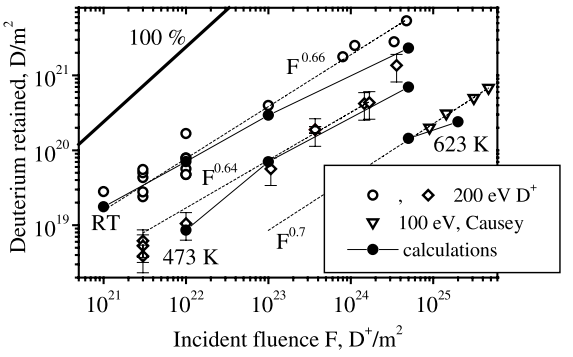

Fig. 3. Fluence dependence of the retained D under the implantation of 200 eV D^+ in PCW at 300 and 473 K. Data by Causey co-workers [21] of the high flux implantation of 100 eV deuterium and tritium ions from a plasma in PCW at 623 K are shown for comparison. Calculations (solid circles) using the parameters presented in Table 1 are in very good agreement with experiments. 100% retention of non-reflected flux is also shown. The reflection coefficient of 200 eV D^+ from W is $r = 0.56$ [27]. Dashed lines are only to guide the eyes.

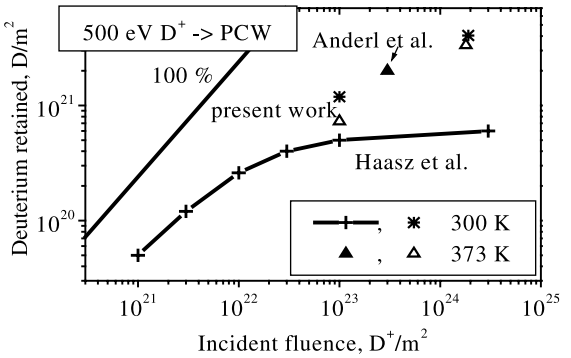

Fig. 4. Comparison with literature data for implantation of 500 eV D^+ in PCW. 100% retention of non-reflected flux is also shown. The reflection coefficient of 200 eV D^+ from W is $r = 0.56$ [27].

in [6,8]. The reason for such disagreement between our data and Haasz et al. [8] is not clear. The saturation behaviour of D retention in PCW with fluence which was reported by Haasz et al. is in disagreement with other data available from the literature [3,6,19,20] and could not be explained using existing models of D migration in metals.

3.1.2. Modelling

The ion beam current was between 40 and 60 μA that is equivalent to a flux density of $I_0 = 2.5 \times 10^{19}$–4×10^{19} D/m^2 s. During the implantation of low-energy D ions, a part of the incident D, rI_0 is reflected from the surface of the pure W with the reflection coefficient $r \approx 0.56$ as calculated with TRIM.SP [27], while the other part, $(1-r)I_0$, is implanted. Deuterium ions penetrating the metal slow down near the surface. The depth distribution of the implanted D was calculated by TRIDYN code [27]. The mean implantation depth is $R_p = 5.6$ nm for 200 eV D and $R_p = 15$ nm for 1 keV. The implanted fraction diffuses in the metal with trapping at different kinds of defects. When a diffusing atom reaches the surface, it can recombine with another D atom at the surface to desorb as a hydrogen molecule. Consequently, the model of D behaviour in W includes the implantation profile, D diffusion, trapping and thermal release of D by recombination on the surface [28]. Diffusion of D is described by the diffusion equation with ion source:

$$\frac{\partial u(x,t)}{\partial t} = \frac{\partial}{\partial x}\left(D\frac{\partial u}{\partial x}\right) + (1-r)I_0\varphi(x), \quad 0 < x < L, \quad (1)$$

where u is the mobile D concentration, $D = D_0 \exp(-E_m/kT)$ is the diffusion coefficient and $\varphi(x)$ is the D implantation profile which is taken from TRIDYN calculations [27].

Trapping of D in bcc metals is described by the trapping equation [29]

$$\partial Y(x,t)/\partial t = (2Da/3)(u(W-Y) - (12Y/a^3)\exp(-E_b/kT)), \quad (2)$$

where a is the lattice constant; Y is the trapping concentration; W is the density of traps and E_b is the binding energy of D with a trap defined as the difference of the D energy to be in a trap site and in a solution site. The trapping energy is defined as the energy to release the D atom from a defect: $E_t = E_b + E_m$.

The boundary conditions on the front ($x = 0$) and the back ($x = L$) sides consider D desorption in molecular form and are given by the balances of fluxes [28]:

$$\lambda\partial u(x,t)/\partial t = -J_{0,L} + D\partial u/\partial x + (1-r)I_0\varphi(x)\lambda, \quad x = 0, L, \quad (3)$$

where $\lambda = a/(2\sqrt{2})$ is the jumping distance and J_0 and J_L are the re-emission and permeation fluxes, respectively. The re-emission and permeation rates are

$$J_{0,L} = -2K_r^{0,L}u_{0,L}^2 \quad (\text{atoms m}^{-2}\,\text{s}^{-1}), \quad (4)$$

where K_r is the recombination coefficient which is defined as [30]

$$K_r = s_0 \exp(-2E_c/kT)\mu/K_s^2, \quad (5)$$

where K_s is the solubility [26], $\mu = 1/\sqrt{2\pi mkT}$ (m is the mass of the hydrogen molecule, T is the temperature and k is Boltzmann's constant) and E_c is the surface barrier which according to [31] is zero for hydrogen on pure W. The surface barrier can increase in the presence of

Table 1
Parameters of hydrogen in tungsten for diffusion model

Diffusivity [26], $D = D_0 \exp(-E_m/kT)$		Recombination coefficient [30,31], $K_r = K_{r0} \exp(-E_r/kT)$		Trapping parameters [present work]	
D_0 (m^2/s)	E_m (eV)	K_{r0} (m^4/s)	E_r (eV)	W_t (at.fr.)	E_t (eV)
4.1×10^{-7}	0.39	$3 \times 10^{-25}/T^{1/2}$	−2.06	Intrinsic traps: 4×10^{-4} Ion-induced: Eq. (7), $W_m = 0.1$	Intrinsic traps: 0.85 Ion-induced: 1.45

impurities such as oxygen, carbon or sulfur on a metal surface.

The data for diffusion and recombination coefficients are summarized in Table 1.

To describe the D retention in PCW, two kinds of traps were introduced:

(i) low-temperature traps: intrinsic defects with a trapping energy of 0.85 eV distributed over the whole sample thickness and
(ii) high-temperature traps: 'ion-induced' traps with a trapping energy of 1.45 eV which form and grow during implantation, distributed near the surface and correlated with the implantation range.

The low-temperature traps are associated with natural traps (dislocations, grain boundaries, some impurities, presence of bulk oxide) which are always present in PCW. Both (i) the increase of the temperature and time of W annealing before implantation and (ii) the pre-implantation of W by low-energy D ions at high temperature decrease the concentration of the natural defects (0.85 eV) because of the removal of residual stresses, some impurities and dislocations in the near the surface and the reduction of the dislocation content in the bulk.

The high-temperature traps (1.45 eV) can be associated with D agglomeration in molecules and bubbles near the implanted surface and D trapping in vacancies. The concentration of ion-induced traps increases with (i) the D pre-implantation of W, (ii) the incident ion energy and (iii) the fluence. The binding energy of D in bubbles (about 1 eV) is similar to the measured heat of chemisorption [31], that indicates the same mechanism of D trapping in bubbles as chemisorption on a surface.

Fig. 5 shows a comparison of the model calculations using the parameters given in Table 1 with experimental thermodesorption spectra of 200 eV D^+ implanted at room temperature in PCW for two different fluences. There are two peaks: a low-temperature peak with a maximum about 450 K and a high-temperature peak with a maximum about 600–650 K. The position of the maximum can be changed with experimental heating rate, implantation energy and fluence.

Although the D ion energy (200 eV) is too low to create any elastic-collision defects by displacement of W

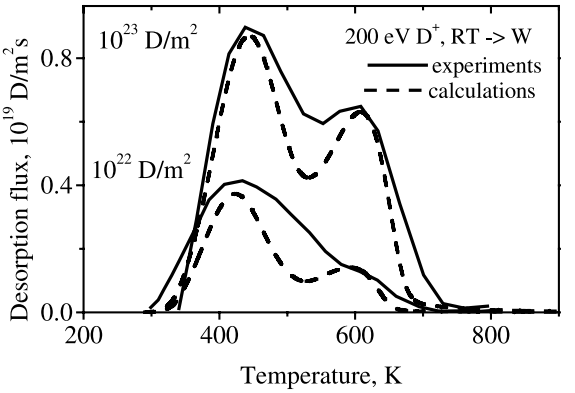

Fig. 5. Experimental thermodesorption spectra (solid lines) for PCW for two different fluences. Calculations (dashed lines) using the parameters presented in Table 1 are in good agreement with experiments.

atoms, the D retention in PCW cannot be explained without taking into account the presence of a high defect concentration in the implantation zone. Since this kind of defects cannot be classified as displacement damage such as vacancies, these defects should involve D bubble formation. The concentration of ion-induced traps (1.45 eV) can increase with fluence and incident energy of implanted D according to

$$dW/dt = (1 - r)I_0\psi(x)\eta(1 - W/W_m), \quad (6)$$

where ψ is the depth distribution of ion-induced defects, η is the speed of the defect creation and W_m is the maximal defect concentration. From Eq. (6) the trap density increases with time, t, as follows:

$$W(x,t) = W_m(1 - \exp(-(1 - r)I_0\psi(x)\eta t/W_m)). \quad (7)$$

The evaluation of the defects with fluence for the implantation of 200 eV D^+ in PCW is shown in Fig. 6. The speed of the trap production increases with the increase of the implantation energy and depends on the microstructure, impurities and lattice imperfections which can create the conditions for D agglomeration in bubbles. According to Sakamoto et al. [13], the vacancy concentration reaches a saturation about 10^{-3} at.fr. at

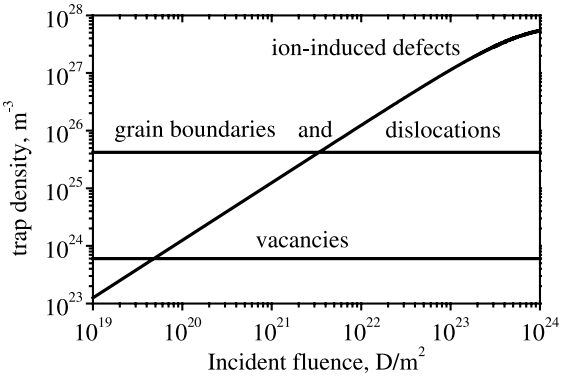

Fig. 6. Calculated evaluation of defects in W with fluence.

fluences above 10^{21} ions/m^2. As follows from the calculations, the concentration of ion-induced traps goes up to 10^{-1} at.fr. or can be even higher. This is another argument that ion-induced traps cannot be a vacancy type of traps but the D agglomeration in bubbles.

Deuterium molecules in the implantation range were observed by Alimov et al. [3]. It is interesting to mention that Alimov et al. have seen molecules in the implantation range for both PCW and single crystal W (SCW). Moreover, Alimov et al. found that in SCW the retained D in molecular form is two times higher than in atomic form. If TDS of the D retention in PCW has two peaks, low- and high-temperature, while TDS for SCW has only one high-temperature peak [32] (Fig. 7). This is because the SCW has much less intrinsic defects like dislocations, grain boundaries and impurities which can trap D in the low-temperature peak. Haasz and coworkers [32] observed higher retention in SCW at low fluences compared to PCW (Fig. 7). This means that the speed of ion-induced trap creation is higher in SCW

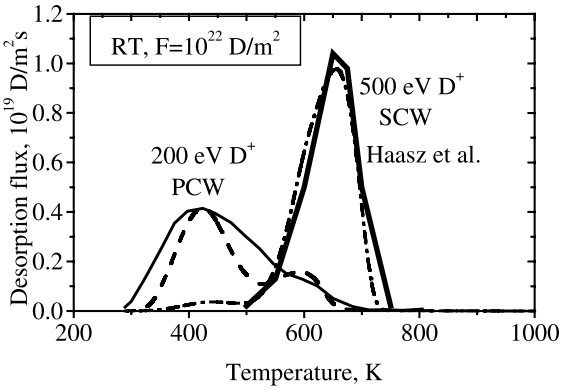

Fig. 7. Thermodesorption spectra (solid lines) for PCW [present work] and for SCW [32]. Calculations (dashed lines) using the parameters presented in Table 1 are in good agreement with both experiments.

($\eta = 10^{-1}$) than in PCW ($\eta = 10^{-3}$). The reason is not yet clear.

Calculations of the fluence dependence and temperature dependence of the D retention using Eqs. (1)–(7) with the parameters presented in Table 1 show a good agreement with experiments (Fig. 3).

3.2. D^+ implantation into W pre-implanted by carbon ions

If carbon is used in a fusion reactor, it can result in carbon deposition on W. Reliable data on the hydrogen isotope behaviour in tungsten–carbon are important for the prediction of tritium uptake and retention in the components of a fusion reactor.

It is clear that the creation of a carbon layer on top of W will result in the D retention in carbon. To understand the influence of a small amount of carbon and formation of carbides on D behaviour in W, carbon ions with an energy of 1 keV have been implanted in W up to a fluence of $F = 5 \times 10^{21}$ C/m^2. The implantation of such a small amount of carbon results in the creation of a mixed W/C layer with a thickness of 20 nm near the surface as it was measured by Rutherford backscattering spectroscopy (RBS) using $^7Li^{2+}$ with 3 MeV energy.

The ion implantation was carried out in the following way:

1. PCW foil was heated at 1573 K for 3 h in vacuum with a background pressure of $p = 2 \times 10^{-4}$ Pa,
2. PCW was outgased for 10 min. at 1273 K in the implantation chamber with a background pressure of $p = 10^{-6}$ Pa before the carbon implantation,
3. implantation of carbon ions with an energy of 1 keV in W at room temperature up to a fluence of $F = 5 \times 10^{21}$ C/m^2,
4. annealing of the sample up to 1273 K for 3 min in the implantation chamber,
5. implantation of 200 eV D ions at room temperature.

For every new measurement new PCW foil was used.

Implanted 200 eV D ions will stop within the carbon modified layer. At low fluences, the amount of D retained in W/C by implantation of 200 eV D^+ is higher than that in pure W (Fig. 8). At high fluences, the W/C layer is eroded by bombardment and the D retention approaches the retention observed in pure W.

Both the increase of the trap concentration and the reduction of the recombination coefficient result in the increase of the D retention. To clarify if the carbon preimplantation results in an increase of the trap concentration, in addition to TDS, D(^{3}He, p)^{4}He nuclear reaction analysis (NRA) technique using ^{3}He ions with 1 MeV energy has been used. The implanted specimens were transported through air to the ion beam analysis chamber. The protons from the nuclear reaction were

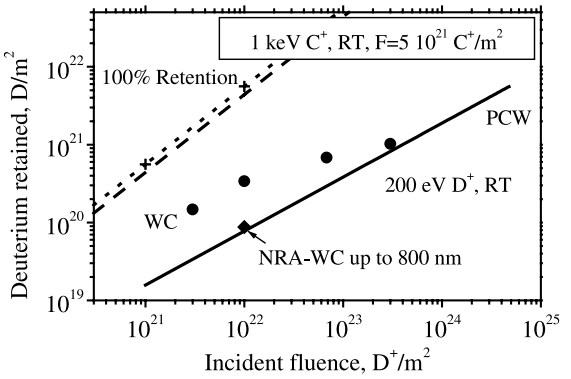

Fig. 8. Fluence dependence of the retained D in pure PCW (solid line) and PCW pre-implanted by 1 keV C^+ at room temperature up to a fluence 5×10^{21} C/m^2 (solid circles). 100% retention of non-reflected flux for PCW (dashed line) and for W/C (doted line with cross) are also shown. The reflection coefficient of 200 eV D^+ from W is $r = 0.56$ and from W/C is $r = 0.44$ [27].

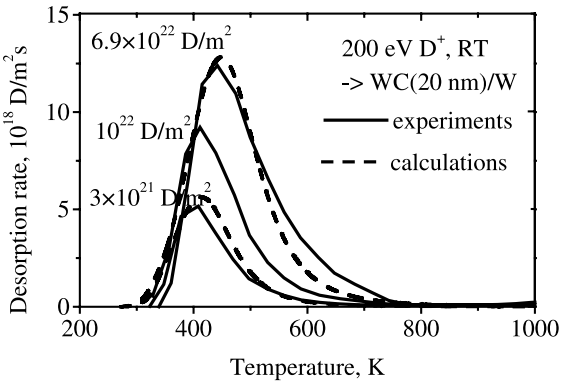

Fig. 9. Experimental thermodesorption spectra (solid lines) for W pre-implanted by 1 keV C^+ at room temperature up to a fluence 5×10^{21} C/m^2 and then implanted by 200 eV D ions at room temperature for various fluences. Calculations (dashed lines) using Eqs. (1)–(7) with the recombination coefficient for WC $K_r = 3 \times 10^{-25} \exp(-0.2/kT)/T^{1/2}$ are also shown.

detected with a large angle counter. Using NRA the D concentration up to a depth of 800 nm was measured. NRA measurements show (Fig. 8) that the concentration of D within the depth of 800 nm is less than the total D concentration measured by TDS. This means that most of the D diffuses far beyond the carbon modified layer (20 nm) and is trapped in natural defects of pure W. Consequently, carbon pre-implantation cannot strongly influence the trap density but significantly decreases the recombination coefficient. As was mentioned above, the presence of impurities on the surface increases the surface barrier. Using a surface barrier of $E_c = 1.1$ eV, the recombination coefficient is $K_r = 3 \times 10^{-25} \exp(-0.2/kT)/T^{1/2}$. Calculations using this recombination coefficient are in a good agreement with TDS of D from W pre-implanted by carbon ions (Fig. 9). TDS shows that the major amount of D is released from W/C at around 400 K. This is the same kind of intrinsic traps as for pure W. Consequently, carbon pre-implantation results in a reduction of the recombination coefficient that increases the solute concentration of D and, from this, D trapping in natural traps in PCW. The high-temperature peak which is due to D agglomeration in bubbles is absent. This means that in W/C deuterium is retained only in atomic form. This is in agreement with [3] where molecules were not detected in carbon deposited W. The conclusions are

– same intrinsic trapping sites in WC as in pure W;
– no molecule formation was observed in WC;
– pre-implantation with C^+ decreases the D recombination coefficient, and, consequently, increases the amount of retained D.

3.3. D^+ implantation into WO_3

Before oxidation, the PCW was heated at 1573 K for 3 h in a vacuum with a background pressure of $p = 2 \times 10^{-4}$ Pa. The formation of the oxide films on PCW has been done by two different methods: (i) by annealing in air at 673 K and (ii) by evaporation of tungsten oxide granules of purity >99.99% on PCW using electron beam deposition. The evaporation rate of WO_3 was about 20 nm/min. RBS showed that the thickness of the tungsten oxides was varied from 100 to 400 nm depending on the time of heating in air or the time of evaporation. X-ray diffraction (XRD) measurements showed that the structure of the oxide films grown in air is crystalline tungsten trioxide. The most intensive peaks in XRD pattern can be related to cubic modification. Therefore, the crystalline tungsten trioxide is assumed to be formed dominantly on the basis of cubic phase WO_3. The structure of the oxide films produced by evaporation from tungsten oxide is the amorphous tungsten trioxide. However, the heating of WO_3/PCW for 3 min up to 873 K in the implantation chamber for outgasing results in a change of the amorphous WO_3 to the crystalline WO_3. This is a reason that the same D retention was observed for both kinds of films.

Fig. 10 demonstrates the fluence dependence of the retained D in pure PCW and WO_3/PCW under the implantation of 200 eV D ions at room temperature. The D retention is strongly increased in WO_3. At low fluences, all implanted D is retained in WO_3. NRA indicates that most of the D is accumulated in the bulk of the W far beyond the implantation range and is captured by traps. The prolonged irradiation with 200 eV D^+ results in the reduction of WO_3 to lower oxides and eventually to

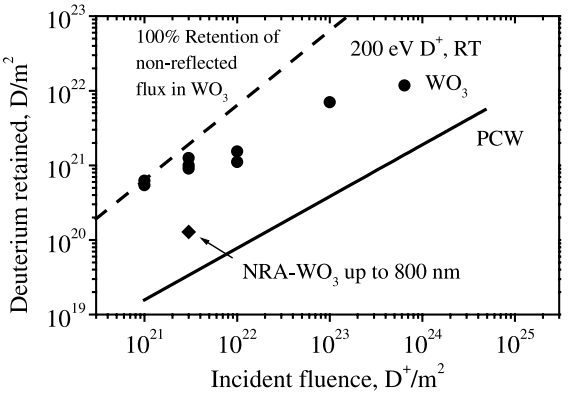

Fig. 10. Fluence dependence of the retained D in pure PCW (solid line) and WO_3 on PCW (solid circles) for implantation of 200 eV D ions at room temperature. 100% retention of non-reflected flux of 200 eV D ions implanted in WO_3 (dashed line) is also shown. The reflection coefficient of 200 eV D^+ from WO_3 is $r = 0.36$ [27].

metallic PCW because of preferential sputtering of the oxygen atoms from the surface.

4. Summary and recommendations for future work

Ion-driven D retention in PCW has been investigated for various energies of implantation, temperatures, fluences and surface conditions. The main conclusions are

- D retention increases slightly faster than the square root of the fluence,
- D retention decreases with increasing temperature,
- D is retained far beyond the implantation range at RT in PCW,
- D is retained both as atoms and as molecules,
- pre-annealing at 1573 K results in a decrease of the D retention,
- pre-implantation of 1 keV C^+ at room temperature and low fluence (i) increases the D retention and (ii) prevents the D bubble formation,
- D retention is strongly increased in WO_3/W compared to pure W,
- A model including two kinds of traps describes well most of experiments in PCW:
  (a) trap energy of 0.85 eV – intrinsic defects (dislocations, grain boundaries, impurities),
  (b) trap energy of 1.45 eV – ion-induced defects (D agglomeration in bubbles).

  The following points require future studies:

- defect creation by neutron irradiation,
- correlation between blistering, substrate temperature and D retention.

Acknowledgements

We would like to thank A. Weghorn for the technical assistance, S. Lindig for SEM, J. Perchermeier and A. Wiltner for the preparing of the tungsten oxide. We are grateful to R.G. Macaulay-Newcombe, R. Causey, M. Balden, H. Maier, V. Alimov and C. Linsmeier for helpful discussions.

References

[1] V.Kh. Alimov, B.M.U. Scherzer, J. Nucl. Mater. 240 (1996) 75.
[2] V.Kh. Alimov, K. Ertl, J. Roth, J. Nucl. Mater. 290–293 (2001) 389.
[3] V.Kh. Alimov, A.P. Zakharov, R.Kh. Zalavutdinov, in: A. Hassanein (Ed.), Hydrogen and Helium Recycling at Plasma Facing Materials, NATO Science Series, vol. 54, 2001, p. 131.
[4] C. Garcia-Rosales, P. Franzen, H. Plank, J. Roth, E. Gauthier, J. Nucl. Mater. 233–237 (1996) 803.
[5] P. Franzen, C. Garcia-Rosales, H. Plank, J. Roth, V.Kh. Alimov, J. Nucl. Mater. 241–243 (1997) 1082.
[6] R.A. Anderl, R.J. Pawelko, S.T. Schuetz, J. Nucl. Mater. 290–293 (2001) 38.
[7] A.A. Pisarev, A.V. Varava, S.K. Zdanov, J. Nucl. Mater. 220–222 (1995) 926.
[8] A.A. Haasz, J.W. Davis, M. Poon, R.G. Macaulay-Newcombe, J. Nucl. Mater. 258–263 (1998) 889.
[9] A. Haasz, M. Poon, J. Davis, J. Nucl. Mater. 266–269 (1999) 520.
[10] M. Poon, R.G. Macaulay-Newcombe, J.W. Davis, A.A. Haasz, J. Nucl. Mater. 307–311 (2002) 723.
[11] R. Causey, K. Wilson, T. Venhaus, W.R. Wampler, J. Nucl. Mater. 266–269 (1999) 467.
[12] T. Venhaus, R. Causey, R. Doerner, T. Abeln, J. Nucl. Mater. 290–293 (2001) 505.
[13] R. Sakamoto, T. Muroga, N. Yoshida, J. Nucl. Mater. 220–222 (1995) 819.
[14] H. Iwakiri, K. Morishita, N. Yoshida, J. Nucl. Mater. 307–311 (2002) 135.
[15] M. Poon, J. Davis, A.A. Haasz, J. Nucl. Mater. 283–287 (2000) 1062.
[16] V.Kh. Alimov, K. Ertl, J. Roth, K. Schmid, J. Nucl. Mater. 282 (2000) 125.
[17] S. Nagata, K. Takahiro, Physica Scripta T 94 (2001) 106.
[18] H. Eleveld, A. van Veen, J. Nucl. Mater. 191 (1992) 433.
[19] A. van Veen, H.A. Filius, J. de Vries, K.R. Bijkerk, G.J. Rozing, D. Segers, J. Nucl. Mater. 155–157 (1988) 1113.
[20] W. Wang, J. Roth, S. Lindig, C.H. Wu, J. Nucl. Mater. 299 (2001) 124.
[21] T. Venhaus, T. Abeln, R. Doerner, R. Causey, J. Nucl. Mater. 290–293 (2001) 505.
[22] F.C. Sze, L. Chousal, R.P. Doerner, S. Luckhardt, J. Nucl. Mater. 266–269 (1999) 1212.
[23] F.C. Sze, L. Chousal, R.P. Doerner, S. Luckhardt, J. Nucl. Mater. 246 (1997) 165.

[24] F.C. Sze, R.P. Doerner, S. Luckhardt, J. Nucl. Mater. 264 (1999) 89.
[25] W. Eckstein, C. Garcia-Rosales, J. Roth, W. Ottenberger, Sputtering data, Tech. Rep. IPP 9/82, Max-Planck-Institut fuer Plasmaphysik, 1993.
[26] R. Frauenfelder, J. Vac. Sci. Technol. 6 (1968) 388.
[27] W. Eckstein, Computer Simulation of Ion-Solid Interaction, Springer, Berlin, 1991.
[28] O.V. Ogorodnikova, M.A. Fuetterer, E. Serra, G. Benamati, J.-F. Salavy, G. Aiello, J. Nucl. Mater. 273 (1999) 66.
[29] O.V. Ogorodnikova, in: A. Hassanein (Ed.), Hydrogen and Helium Recycling at Plasma Facing Materials, NATO Science Series, vol. 54, 2001, p. 7.
[30] M.A. Pick, K. Sonnenberg, J. Nucl. Mater. 131 (1985) 208.
[31] P.W. Tamm, L.D. Schmidt, J. Chem. Phys. 51 (12) (1969) 5352.
[32] R.G. Macaulay-Newcombe, A.A. Haasz, M. Poon, J.W. Davis, in: A. Hassanein (Ed.), Hydrogen and Helium Recycling at Plasma Facing Materials, NATO Science Series, vol. 54, 2001, p. 145.